bioRxiv preprint doi: https://doi.org/10.1101/462929; this version posted November 5, 2018. The copyright holder for this preprint (which was not certified by peer review) is the author/funder, who has granted bioRxiv a license to display the preprint in perpetuity. It is made available under aCC-BY 4.0 International license.

A more physiological approach to lipid metabolism alterations in cancer: CRC-like organoids assessment

Silvia Cruz-Gil[1], Dr. Ruth Sanchez-Martinez[1], Sonia Wagner-Reguero[1], Dr. Daniel Stange[2], Dr. Sebastian Schölch[3,4,5], Dr. Kristin Werner[2] and Dr. Ana Ramirez de Molina[1,*].

[1] Molecular Oncology Group/ IMDEA Food Institute, CEI UAM + CSIC, Ctra. De Cantoblanco, 8 E-28049 Madrid, Spain.

[2] Department of Gastrointestinal, Thoracic and Vascular Surgery, University Hospital Carl Gustav Carus, Technische Universität Dresden, Fetscherstraße 74, 01307 Dresden, Germany.

[3]Medizinische Fakultät und Universitätsklinikum Mannheim, Ruprecht-Karls-Universität Heidelberg, Theodor-Kutzer-Ufer 1-3, 68167 Mannheim

[4]German Cancer Consortium (DKTK)

[5]German Cancer Research Center (DKFZ), Heidelberg, Germany

[*]Correspondence to Dr. Ana Ramirez de Molina. (E-mail: ana.ramirez@imdea.org).

Running head

Handling organoids for an optimal lipid metabolism-related CRC analysis.

bioRxiv preprint doi: https://doi.org/10.1101/462929; this version posted November 5, 2018. The copyright holder for this preprint (which was not certified by peer review) is the author/funder, who has granted bioRxiv a license to display the preprint in perpetuity. It is made available under aCC-BY 4.0 International license.

Abstract

Precision medicine might be the response to the recent questioning of the use of metformin as an anticancer drug in colorectal cancer (CRC). Thus, in order to establish properly its benefits, its application need to be assayed on the different progression stages of CRC. In this way, organoids imply a more physiological tool, representing a new therapeutic opportunity for CRC personalized treatment to assay tumor stage-dependent drugs effects. Since the lipid metabolism-related axis, ACSL/SCD, stimulates colon cancer progression and Metformin is able to rescuing the invasive and migratory phenotype conferred to cancer cells upon this axis overexpression; we checked ACSL/SCD status, its regulatory miRNAs and the effect of Metformin treatment in organoids as a model for specific and personalized treatment. Despite ACSL4 expression is upregulated in CRC-like organoids, Metformin is able to downregulate it, especially in the first stages. Besides, organoids are clearly more sensitive in this first stage (Apc mutated) to Metformin than current chemotherapeutic drugs such as fluorouracil (5-FU). Metformin performs an independent "Warburg effect" blockade to cancer progression and is able to reduce crypt stem cell markers expression such as Lgr5+. These results suggest a putative increased efficiency of the use of Metformin in the first stages of CRC than in advanced disease.

Keywords: CRC-like organoids, colorectal cancer, ACSL/SCD axis, lipid metabolism, acyl-CoA synthetases, Stearoyl-CoA desaturase, Metformin, LGR5+, non-Warburg metabolism, personalized medicine.

Abbreviations: ACSL1: Acyl-CoA synthetase 1; ACSL4: Acyl-CoA synthetase 4; CRC: Colorectal cancer; EMT: Epithelial-mesenchymal transition; 5-FU: Fluorouracil; MiRNAs/ miR: MicroRNAs; MTT: 3-(4, 5-dimethylthiazol-2-yl)-2, 5-diphenyltetrazolium bromide; OAA: Oxaloacetate; SCD: Stearoyl-CoA desaturase; TCA: Tricarboxylic Acid cycle; 2D: 2-dimensional; 3D: 3-dimensional.

bioRxiv preprint doi: https://doi.org/10.1101/462929; this version posted November 5, 2018. The copyright holder for this preprint (which was not certified by peer review) is the author/funder, who has granted bioRxiv a license to display the preprint in perpetuity. It is made available under aCC-BY 4.0 International license.

Introduction

Colorectal cancer (CRC) is the third most common cancer in men (10% of the total), after lung and prostate cancer, and the second in women (9.2% of the total), after breast cancer [1]. Most of the CRC cases are sporadic (70-80%), which consists of the acquisition of somatic mutations and in which there is no family history or genetic predisposition. The remaining cases (20-30%) are those among close relatives, which are divided into inherited or familial CRC, [2]. Genetically, sporadic CRC development is due to the abnormalities accumulation in tumor suppressor genes and oncogenes [3,3]. Previous research postulated the adenoma-carcinoma transition theory, in which specific somatic mutations promoting tumorigenesis are acquired; proposed by Fearon and Vogelstein (Vogelgram). The Vogelgram proposes that the adenoma-carcinoma sequence model would start with loss of the *APC* gene, followed by mutations in *KRAS* or *BRAF* genes, mutations or loss of *TP53* gene and of SMAD family member 4 (*SMAD4*) [4].

Over the last decade, the interest in metabolic research with respect to cancer has been expansively increased. The first and most characterized tumor metabolism event to be described is the exacerbated glucose uptake and glycolysis utilization; which even in normoxic condition, are not used for maximal ATP generation via mitochondrial respiration. This phenomenon is denoted as the “Warburg effect”.

Even though lipid-associated pathways are functionally dependent on glucose and glutamine catabolic pathways, are now a well-recognized and frequently described cancer metabolic feature with a key role in their tumorigenesis. This is the case for the ACSL/SCD axis [5], a lipid metabolism-related network described to promote tumorigenesis through an epithelial-mesenchymal transition (EMT) program that promotes migration and invasion of colon cancer cells. The mesenchymal phenotype produced upon overexpression of these enzymes is reverted through reactivation of AMPK signaling performed by the well-known anti-diabetic drug, Metformin. Though its mechanism of action is not fully understood, Metformin has shown a

bioRxiv preprint doi: https://doi.org/10.1101/462929; this version posted November 5, 2018. The copyright holder for this preprint (which was not certified by peer review) is the author/funder, who has granted bioRxiv a license to display the preprint in perpetuity. It is made available under aCC-BY 4.0 International license.

robust anti-proliferative effect on several types of cancer such as colon, pancreatic, breast, ovarian, prostate and lung cancer cells [6]. Furthermore, Metformin has been recently associated with improved survival of cancer patients, including CRC, though its use as an antitumoral agent has not been established yet [7]

The ACSL/SCD axis pro-tumorigenic activity has been also described to be post-transcriptionally regulated by miRNAs. miR-544a, miR-142, and miR-19b-1 has been proposed as major regulators of the ACSL/SCD network and the miR-19b-1-3p isoform decreased expression associated with a poorer survival rate in CRC patients, consistently with ACSL/SCD involvement in patients relapse [8].

To get insight into the metabolic implication on CRC progression with a special focus on the ACSL/SCD axis and the effect of metformin in each case, more personalized and physiological tools are needed since most of the available data rely on traditional studies using cancer cell lines cultures. In this way, the organoid culture system opens a new methodological door for *ex vivo* studies.

Adult tissue-derived epithelial organoids, also called “mini guts” [9] are stereotypic tissue-like structures derived from digestive healthy tissues or tumors which mimics *in vitro* the tissue composition and morphology of their *in vivo* counterparts [10]. This methodology was first established in long-term primary culture from mouse small intestinal crypts to generate epithelial organoids with crypt- and villus-like epithelial domains representing both progenitor and differentiated cells [11].

The organoids technology takes advantage of the intestinal epithelium self-renewing capacity. Organoids starts from LGR5+ gut epithelial stem cells forming symmetric cyst structures, which finally will form budding structures resembling intestinal crypts. These budding structures are formed by these LGR5+ stem cells flanked by differentiated daughter cells [9].

bioRxiv preprint doi: https://doi.org/10.1101/462929; this version posted November 5, 2018. The copyright holder for this preprint (which was not certified by peer review) is the author/funder, who has granted bioRxiv a license to display the preprint in perpetuity. It is made available under aCC-BY 4.0 International license.

94 Organoids are currently employed in colorectal cancer studies and chemotherapy assessment
95 [12,13]. Along with intestinal organoids, similar epithelial organoids culture conditions for other
96 mouse and human digestive epithelial tissues have been also adapted [14–17] including tumor-
97 derived organoids from cancer patients. Importantly, organoids grow as pure epithelial cultures
98 without any contamination of vessels, immune cells or non-transformed mesenchymal which
99 leads to an accurate sequencing or expression profiling [10].
100

bioRxiv preprint doi: https://doi.org/10.1101/462929; this version posted November 5, 2018. The copyright holder for this preprint (which was not certified by peer review) is the author/funder, who has granted bioRxiv a license to display the preprint in perpetuity. It is made available under aCC-BY 4.0 International license.

Materials and Methods

CRC-like organoids: culture and maintenance

Mice: Mutant intestinal murine organoids were obtained from the Universitätsklinikum Carl Gustav Carus, Dresden. All procedures involving animals were conducted strictly in accordance with FELASA regulations and approved by the animal welfare committees of the Technische Universität Dresden and the Landesdirektion Sachsen prior to initiation of the experiments.

Mice with conditional mutations in Apc, Kras, Tp53 and Smad4 were obtained from the NCI Mouse Repository (Apc, Kras Tp53) or the Jackson Laboratory (Smad4) and interbred to obtain compound mutant mice (Table 1). The CRC-like organoid model represents the adenoma-carcinoma sequence with the most common acquired mutations in a sporadic CRC: $APC^{fl/fl}$, $KRAS^{G12D/WT}$, $P53^{R172H/WT}$ and $Smad4^{fl/fl}$ (corresponding to stages I to IV) (Table 2). The parental mouse lines were described in Table 2.

Table 1: Parental mouse lines and publication´s PMID of the mutations in the organoids

Mutation	Designation	PMID
APC	NCI: 01XAA	17002498
KRAS ^{G12D}	JAX: 008179	11323676
P53 ^{R172H}	JAX: 008652	15607980
P53 floxed	NCI: 01XC2	11694875
Smad4 floxed	JAX: 017462	11857783

Table 2: CRC-like organoids with the acquired mutations related to the stage.

Organoid mutation	CRC-like stage
WT	-
$APC^{fl/fl}$	I
$APC^{fl/fl}$, $KRAS^{G12D/WT}$	II
$APC^{fl/fl}$, $KRAS^{G12D/WT}$,$P53^{fl/R172H}$	III
$APC^{fl/fl}$, $KRAS^{G12D/WT}$,$P53^{fl/R172H}$,$Smad4^{fl/fl}$	IV

bioRxiv preprint doi: https://doi.org/10.1101/462929; this version posted November 5, 2018. The copyright holder for this preprint (which was not certified by peer review) is the author/funder, who has granted bioRxiv a license to display the preprint in perpetuity. It is made available under aCC-BY 4.0 International license.

Murine organoids mutagenesis is conditioned by the Cre/loxP system. Adenoviral infections were performed as explained in [18] to provide active mutations.

Crypt isolation and organoid culture: Crypts were isolated from the murine small intestine by incubation for 30 min at 4°C in PBS containing 2 mM EDTA as previously reported [11,19]. Isolated crypts were seeded in Matrigel (Corning® Matrigel® Matrix). The basic culture medium (Advanced Dulbecco's modified Eagle Medium DMEM/F12 complemented with penicillin/streptomycin, 10 mmol/L HEPES, 1x Glutamax [Gibco], named ADF +++) was supplemented with: 100 ng/ml Noggin (Peprotech), R-spondin (conditioned medium, 10% final volume), 1x B27 (Invitrogen), 1x N2 (Invitrogen), 1,25 mM N-acetylcysteine (Sigma-Aldrich), 100 µg/mL Primocin TM (InvivoGen) and 50 ng/mL mEGF (Thermofisher). The complete media is named supplemented ADF +++ media. For passaging, organoids were removed from Matrigel and mechanically dissociated with a glass pipette, pelleted and then transferred to fresh Matrigel [11,14,20]. Splitting was performed twice a week in a 1:3 split ratio. Cultures were kept at 37 °C, 5% CO2 in humidity.

Drugs treatment - viability assays

Cell viability was determined by counting and seeding 1000 crypts in 60% of Matrigel in 48-well plates. After 2 days of culture, organoids were exposed 48 hours to 10 µM Metformin (Sigma) or 10, 100 or 150 µM 5-FU (Sigma) in supplemented ADF +++ media, as indicated in the figures. At this point, organoids were collected, split and reseeded for recovery experiments over 72 hours in supplemented ADF +++ media.

Upon treatments (48h) or recovery assays (post-72h), organoids were incubated 3 hours with 3-(4,5-dimethyl-thyazol-2-yl)-2,5-diphenyl-tetrazolium (MTT, Sigma). After discarding the media, 20 µl of 2% SDS (Sigma) solution in H2O was added to solubilize Matrigel (2 h, 37 °C). The

bioRxiv preprint doi: https://doi.org/10.1101/462929; this version posted November 5, 2018. The copyright holder for this preprint (which was not certified by peer review) is the author/funder, who has granted bioRxiv a license to display the preprint in perpetuity. It is made available under aCC-BY 4.0 International license.

resultant formazan was dissolved in 100 µl of DMSO for 1 h (37 °C). The absorbance was measured on the microplate reader (Asys UVM 340, Isogen life science) at 562 nm.

Untreated organoids were defined as 100% viable. Data were expressed as the fold change of viable cells from treated organoids compared to the non-treated organoids.

RNA isolation and RT-QPCR

For RNA isolation, organoids were released from Matrigel (Corning) with cold Dispase (Corning) and pelleted by centrifugation. The supernatant was removed and pelleted organoids were carefully resuspended in Trizol (Qiagen), and storage at -80ºC. RNA was isolated according to the supplier's protocol (Invitrogen) and the concentration and purity (A260/A280 ratio) were determined by spectrophotometric analysis (NanoDrop 2000 Spectrophotometer ThermoScientific). 20 ng/µl RNA was reverse-transcribed using the High Capacity RNA-to-cDNA kit (ThermoFisher), according to manufacturer's instructions. Relative gene expression was measured using VeriQuest Fast SYBR Green qPCR Master Mix (2X) (Isogen). Primers used are listed in S1 Table. Regarding miRNAs, their expression was monitored using TaqMan® MicroRNA Reverse Transcription Kit (ThermoFisher Scientific) and Taq-man miRNA probes for RT-qPCR (S2 Table). RT-QPCRs were performed on the QuantStudio 12K Flex (Applied Biosystems) and the $2^{-\Delta\Delta Ct}$ method was applied to calculate the relative gene or miRNA expression.

L-Lactate quantification

Organoids were seeded at a density of 1000 crypts per well in a 48-well plate. After 48 hours, the medium was changed to PBS, 10 mM of Metformin or 10 µM 5-FU in supplemented ADF +++ media overnight at 37°C before quantification. Using Cayman's Glycolysis cell-based assay (Cayman, Ann Arbor, MI, USA, 600450) extracellular L-Lactate was measured by determining absorbance at 490 nm. L-Lactate measurements (mM) were normalized to total protein concentration (mg) x100.

bioRxiv preprint doi: https://doi.org/10.1101/462929; this version posted November 5, 2018. The copyright holder for this preprint (which was not certified by peer review) is the author/funder, who has granted bioRxiv a license to display the preprint in perpetuity. It is made available under aCC-BY 4.0 International license.

Statistical analysis

All statistical analyses were performed using the Graph Pad Prism software (Ver. 7.03) (GraphPad Software, San Diego, CA, USA). Significance between groups was determined by *t*-test analyses (unpaired Student's t-tests). Data with $P < 0.05$ were considered statistically significant (ns, $P > 0.05$; *, $P \leq 0.05$; **, $P \leq 0.01$; ***, $P \leq 0.001$; ****, $P \leq 0.0001$). All reported *p* values were two-sided. All values are reported as mean ± S.D.

bioRxiv preprint doi: https://doi.org/10.1101/462929; this version posted November 5, 2018. The copyright holder for this preprint (which was not certified by peer review) is the author/funder, who has granted bioRxiv a license to display the preprint in perpetuity. It is made available under aCC-BY 4.0 International license.

Results

ACSL4 is overexpressed throughout CRC-like organoids stages

ACSL4 has been previously reported to be overexpressed in malignant tumors, and together with ACSL1 and SCD form an axis involved in CRC progression. ACSL1, ACSL4, and SCD mRNA expression was measured in CRC-like organoids. ACSL4 mRNA was very significantly augmented in more aggressive stages compared to WT (Fig 1A). It is shown an intermediate expression pattern in Apc-mutated organoids, with a significantly differential expression (*p-value:* **) compared to the following second stage (Apc, Kras mutated stage) henceforth. Conversely, ACSL1 and SCD levels were maintained or increased from the third stage henceforth, respectively (S1 Fig).

Figure 1: ACSL4 is overexpressed throughout CRC-like organoids stages while miR-19b-1-3p preserves its protective role.

A) RT-QPCR analysis showing ACSL4 mRNA expression levels throughout CRC-like organoids stages. B) RT-QPCR analysis showing miR-19b-1-3p mRNA expression levels throughout CRC-like organoids stages. Results represent the fold-change mean ±SD ($n = 4$) in plots A, ($n = 3$) in plots B. (ns, $P > 0.05$; *, $P \leq 0.05$; **, $P \leq 0.01$; ***, $P \leq 0.001$; ****, $P \leq 0.0001$)

Interestingly, organoids in more advanced stages (III and IV) presented a genetic misbalance in ACSL4 expression (Fig 1A) with huge differences in their fold inductions ranges in the same stage, though with a similar tendency.

MiR-19b-1-3p keeps its protective role in CRC-like organoids

MiRNAs expression was assayed in 3 different RNA extractions over time. Previous results from our group pointed toward a correlation between miR-19b-1-3p lower expression and a poorer

bioRxiv preprint doi: https://doi.org/10.1101/462929; this version posted November 5, 2018. The copyright holder for this preprint (which was not certified by peer review) is the author/funder, who has granted bioRxiv a license to display the preprint in perpetuity. It is made available under aCC-BY 4.0 International license.

prognosis in CRC patients (which might have a putative high clinical interest due to its potential to be assed in plasma as a non-invasive biomarker); very likely through its involvement in cell invasion and lipid metabolism regulation [8]. In the case of CRC-like organoids, this tendency was maintained and miR-19b-1-3p expression was decreased in a stage-dependent manner (Fig 1B).

Together with miR-19b-1-3p, miR-142 (3p and 5p isoforms) and miR-544a (without murine isoform) were also involved on targeting ACSL/SCD axis [8]. Hence, the previous mentioned miRs plus miR-19b-1-5p isoform was measured though no statistically significant differences were found in its expression (S2 Fig)

Metformin decreases CRC-like organoids viability to the same extent as current chemotherapy without significant effects on WT organoids

Since Metformin treatment, an AMPK activator used as antidiabetic treatment that has been recently associated to increased survival of cancer patients, was able to rescue the epithelial phenotype from the EMT process caused by the overexpression of ACSL/SCD in CRC cells [5]; we wondered what this drug effect would be through the different stages in tumor progression. CRC-like organoids were treated with PBS, 10 μM of Metformin or with the commonly used chemotherapeutic agent 5-FU; and the organoids viability was examined by MTT assays 48 hours upon treatment. None of the drugs affected significantly the viability of WT organoids (Fig 2A), while they were able to cause a decrease of about 50% in the viability of mutated organoids corresponding to the most aggressive phenotypes (Fig 2B-E). 5-FU higher concentrations (100 μM and 150 μM) showed the same effects than the lower concentration (10 μM) in mutated organoids, while they had stronger effects on WT ones (S3A-E Figs).

Figure 2: Metformin decreases CRC-like organoids viability to the same extent as current chemotherapy without significant effects on WT organoids

bioRxiv preprint doi: https://doi.org/10.1101/462929; this version posted November 5, 2018. The copyright holder for this preprint (which was not certified by peer review) is the author/funder, who has granted bioRxiv a license to display the preprint in perpetuity. It is made available under aCC-BY 4.0 International license.

MTT cell viability assays upon 48 hours treatments with Metformin or 5-FU in the different CRC-like organoids representative stages (A) WT organoids; (B) $APC^{fl/fl}$ organoids resembling stage I; (C) $APC^{fl/fl}$, $KRAS^{G12D/WT}$ organoids resembling stage II; (D) $APC^{fl/fl}$, $KRAS^{G12D/WT}$,$P53^{R172H/WT}$ organoids resembling stage III; (E) $APC^{fl/fl}$, $KRAS^{G12D/WT}$,$P53^{R172H/WT}$,$Smad4^{fl/fl}$ organoids resembling stage IV. Data are represented by the fold-change mean ±SD (n = 3) in all the plots except A: (n=2). (ns, $P > 0.05$; *, $P \leq 0.05$; **, $P \leq 0.01$; ***, $P \leq 0.001$; ****, $P \leq 0.0001$).

Metformin treatment recovery is significantly lower compared to 5FU in first stages organoids while WT organoids present an opposite behavior

To further check the treatments scope, and analyzing not only the effect but also the potential reversibility of the treatment in normal and tumoral cells in different stages, organoids viability was assayed upon 48 hours treatment (PBS, Metformin or 5-FU) plus the subsequent recovery of 72 additional hours in their growing media. In this case, WT organoids showed differential recovery sensitivity to the treatment. Metformin treated and recovered WT organoids presented almost similar measurements than only treated organoids. Nonetheless, 5FU treated WT organoids recoveries are noteworthy more sensitive and upon 72h recovery time their viability was quite significant reduced (*p-value:* ***) (Fig 3A). In Apc mutated organoids the recovery is very significantly lower upon Metformin treatment (*p-value:* ****) than 5-FU (*p-value:* *), compared to PBS recovery control; making these Apc mutated organoids the most responsive to the Metformin treatment compared to 5-FU (Fig 3B). Regarding organoids corresponding to stages II-III (Figs 3C and D), both treatments presented almost similar recovery effects, while in stage IV organoids, 5-FU presented a stronger effect shown by the lower recovery of these 5-FU treated organoids (Fig 3E). Again 5-FU higher concentrations (100 µM and 150 µM) had nearly the same recovery effects than the lower concentration (10 µM) (S4A-E Figs).

bioRxiv preprint doi: https://doi.org/10.1101/462929; this version posted November 5, 2018. The copyright holder for this preprint (which was not certified by peer review) is the author/funder, who has granted bioRxiv a license to display the preprint in perpetuity. It is made available under aCC-BY 4.0 International license.

Figure 3: Metformin treatment recovery is significantly lower compared to 5FU in first stages organoids while WT organoids present an opposite behavior

MTT cell viability assays upon 48 hours treatments (black bars) and upon extra 72h post-treatment recovery with PBS (light grey bars) Metformin (yellow bars) or 5-FU (dark grey bars) in the different CRC-like organoids representative stages (A) WT organoids; (B) $APC^{fl/fl}$ organoids resembling stage I; (C) $APC^{fl/fl}$, $KRAS^{G12D/WT}$ organoids resembling stage II; (D) $APC^{fl/fl}$, $KRAS^{G12D/WT}$,$P53^{R172H/WT}$ organoids resembling stage III; (E) $APC^{fl/fl}$, $KRAS^{G12D/WT}$,$P53^{R172H/WT}$,$Smad4^{fl/fl}$ organoids resembling stage IV. Data are represented by the fold-change mean ±SD (n = 3) in all the plots. (ns, $P > 0.05$; *, $P \leq 0.05$; **, $P \leq 0.01$; ***, $P \leq 0.001$; ****, $P \leq 0.0001$). (F) Organoids pictures with PBS, Metformin or 5-FU, upon 48 hours treatments and upon extra 72h post-treatment recovery as indicated. Pictures were captured using the × 10 objective, in bright field. Leica microscope (Leica microsystems).

Since WT organoids require more time to achieve their size and their crypt-like phenotype (Fig 3F), the recovery measures are lesser than the mutated organoids. On the other hand, WT organoids recovered upon Metformin treatment presented a higher size than the ones treated with 5-FU (Fig 3F). On the contrary, stage I (Apc mutated) organoids recovered upon Met treatment showed an evident reduced size compared with the control and the 5-FU treated ones. In accordance with viability assays results, this effect is lost in further stages; where Metformin is less effective and Metformin treated recovered organoids presented a bigger size than the ones treated with 5-FU.

By way of clarification, all mutated organoids presented Apc mutated since is the first gene in the adenocarcinoma sequence. Apc completed deletion provokes a hyperactive Wnt signaling. This aberration makes an organoids phenotype switch, losing their crypt-like structure and adopting a cystic morphology [17,21]

bioRxiv preprint doi: https://doi.org/10.1101/462929; this version posted November 5, 2018. The copyright holder for this preprint (which was not certified by peer review) is the author/funder, who has granted bioRxiv a license to display the preprint in perpetuity. It is made available under aCC-BY 4.0 International license.

Metformin action is stronger on ACSL4 and SCD overexpressing first stages organoids

Since stage I organoids seemed to present a differential sensitivity to metformin compared to other stages, together with a differential expression of ACSL4, we aimed to analyze the possible link between Metformin and ACSL/SCD axis in intestinal organoids.

To this aim, ACSL4 expression was measured, as well as the other enzymes of the ACSL/SCD metabolic network (ACSL1 and SCD) upon 10 µM Metformin treatment. ACSL4 mRNA expression was strongly reduced by this drug compared to their non-treated controls in stage I and II organoids. By contrast, stage III and IV presented no significance in their reduction or a slight significance, respectively. WT organoids also presented a slight reduction of ACSL4 mRNA upon Metformin treatment (Fig 4B). In addition, SCD expression levels were clearly decreased by Metformin in WT and stage I organoids, while a less marked tendency was found for stage III and IV organoids (Fig 4C). ACSL1 mRNA analysis showed less significant results (Fig 4A) upon Metformin treatment.

Figure 4: Metformin action is stronger on ACSL4 and SCD overexpressing first stages organoids and downregulates stem cell biomarker LGR5 and Wnt target genes expression in all organoid stages.

mRNA expression levels of enzymes related to the ACSL/SCD axis, ACSL4 (A), SCD (B), by RT-QPCR; and expression levels of different stem cell markers, Lgr5 (C), Axin-2 (D) and Ctnnb-1 (E) by RT-QPCR upon PBS (black bars) and 10 uM Metformin (yellow bars). Data are represented by the fold-change mean to each PBS control ±SD ($n = 3$). (ns, $P > 0.05$; *, $P \leq 0.05$; **, $P \leq 0.01$; ***, $P \leq 0.001$; ****, $P \leq 0.0001$).

The expression of these enzymes was also measured upon 10 µM 5-FU treatment. This drug was able to significantly downregulate ACSL4 and SCD mRNA in most of the stages, though no

bioRxiv preprint doi: https://doi.org/10.1101/462929; this version posted November 5, 2018. The copyright holder for this preprint (which was not certified by peer review) is the author/funder, who has granted bioRxiv a license to display the preprint in perpetuity. It is made available under aCC-BY 4.0 International license.

differences were showed between the effects in initial and later stages such as the case for Metformin treatment (S5A-C Figs).

Metformin, but not 5-FU, downregulates stem cell biomarker LGR5 and Wnt target genes expression in all organoid stages

To further assay whether Metformin treatment was targeting the organoids crypts stem cell marker, LGR5; we analyzed its expression together with two other Wnt target genes, Axin2 and Ctnnb-1. Importantly, LGR5 expression was significantly diminished in the whole CRC-like organoids series upon Metformin treatment (Fig 4C) as well as Axin-2 (Fig 4D) and Ctnnb-1 (Fig 4E) mRNAs. Surprisingly, this pattern was not maintained when organoids were treated with 10 μM 5-FU (S5D-F Figs).

Metformin action in CRC-like organoids is not related to a Warburg-effect impairement

The avidity to perform glycolysis even in the presence of oxygen, known as the Warburg effect, is one of the hallmarks of tumors. For this reason, we measured the levels of L-lactate, the end product of glycolysis. CRC-like organoids presented increased glycolysis compared to WT organoids, reflecting an increasing Warburg effect throughout the stages, as expected. Even though 5-FU treatment caused a slight decrease in the glycolytic performance of the mutant organoids (Fig 5), Metformin treatment caused an opposite effect, increasing the glycolytic capacity in all stages, especially in stage I, the most sensitive to the drug. Thus, it seems that Metformin effect on CRC-like organoids viability relies in mechanisms other than preventing pro-tumorigenic Warburg effect, likely through the regulation of lipid metabolism.

Figure 5: Metformin action in CRC organoids is not related to a Warburg-effect impairement

Bars represent the extracellular L-lactate production upon overnight PBS treatment (black bars), Metformin treatment (yellow bars) and 5-FU treatment (grey bars) using the Cayman's Glycolysis cell-based assay. L-lactate production measurement is normalized by total protein content (x100).

bioRxiv preprint doi: https://doi.org/10.1101/462929; this version posted November 5, 2018. The copyright holder for this preprint (which was not certified by peer review) is the author/funder, who has granted bioRxiv a license to display the preprint in perpetuity. It is made available under aCC-BY 4.0 International license.

Data are represented by the fold-change mean ±SD (n = 3) in all the plots. (ns, P> 0.05; *, $P \leq$ 0.05; **, $P \leq 0.01$; ***, $P \leq 0.001$; ****, $P \leq 0.0001$).

Discussion

Organoids seem to represent a good tool to study lipid metabolism [22] and previous studies employing intestinal organoids have linked the critical role of fatty acid metabolism to the intestinal epithelial integrity *in vivo* [23]. Therefore, we propose this system to get insight into cancer progression mechanisms in regards to fatty acid metabolism and therefore, to assay ACSL/SCD protumorigenic axis action in CRC.

We showed that ACSL4 augmented while miR-19b-1-3p diminished its expression, both progressively, in murine CRC-like organoids. Metformin action compared to the chemotherapeutic agent 5-FU, in terms of viability reduction, was similar; although no significant reduction was found in WT organoids viability with any treatment. Stage I organoids were the most susceptible to Metformin action compared to 5-FU; while further stages presented similar or stronger sensitivity to 5-FU, including WT organoids. Besides, Metformin was able to reduce the intestinal crypt stem cell marker LGR5 in all the stages, together with two other Wnt downstream targets, Ctnnb-1 and Axin-2. Finally, we showed that even though the CRC-organoids series present a growing Warburg effect through the stages consistent with increased L-lactate levels; Metformin action on CRC organoids viability was not related to an ablation of Warburg effect.

The individual role of ACSL isoform 1 [24,25] and 4 [24,26] as well as SCD [27–31] in CRC has been extensively reported. Surprisingly, while ACSL4 mRNA levels are clearly increased through the stages in this organoids model, this was not the case for ACSL1, and SCD was only overexpressed in advanced stages. These results differ from previous ones using human CRC cells

bioRxiv preprint doi: https://doi.org/10.1101/462929; this version posted November 5, 2018. The copyright holder for this preprint (which was not certified by peer review) is the author/funder, who has granted bioRxiv a license to display the preprint in perpetuity. It is made available under aCC-BY 4.0 International license.

351 which can be due to differential expression in murine tissues compared to human 2D cultures [5]
352 [8]. Nevertheless, the use of murine organoids allows their genetic engineering and to accurately
353 control the mutations for a better mechanistic characterization, rather than patient tumor-derived
354 biopsies with the high variability that each tumor represent. Thus, our CRC model mimics a
355 sporadic colorectal tumor with the common mutations acquired during the progression of this
356 cancer. Due to the organoids results, the overexpression of the three enzymes could be only
357 present in some punctual tumors. However, the overexpression of ACSL4 is preserved in murine
358 organoids with the acquired CRC most common mutations (Fig 1A), indicating a predominant
359 role of this ACSL/SCD component in these cancer progression aspects. The ACSL4 mRNA huge
360 range of expression considering the most mutated stages (Fig 1A) could be explained since stages
361 III and IV in real tumors present an uncontrolled genetic variability with the accumulation of
362 other undetermined mutations. Organoids would be mimicking these uncontrolled stages,
363 compared to the homogeneity presented in 2D cultures. Conversely, ACSL1 static role (S1A Fig)
364 could be due to a lesser implication in tumor development in this system which can be also
365 explained by the fact that the rodent protein is one residue longer (699 amino acids) than the
366 human protein (698 amino acids), making it necessary to study the extent of this dissimilarity.
367 For its part, SCD overexpression has been mainly reported in mesenchymal tissues, rather than
368 epithelial ones, which are the only scaffold for organoids [32,33] giving a reason for the
369 distinctive results found in these epithelial systems among the first stages (S1B Fig).

370 Regarding miRs expression, miR-19b-1-3p kept its tumor-suppressor role in murine CRC-like
371 organoids, also reported as a good prognosis miRNA, able to target the axis [8]. The immature
372 isoform of miR-19b-1-3p, miR-19b, and other members of the miR-17-92 cluster, where this
373 miRNA is involved, regulate the self-renewal ability of gastric cancer stem cells [34]. The miR-
374 17-92 cluster role is controversial and dependent on the cancer type [35,36]. However, it is
375 interesting the reported role of this miRNA in digestive cancer stem cells, and its role in CRC
376 stem cells may be a potential line of research henceforth. In line with our results, miR-19b was
377 also reported to downregulate suppressor of cytokine signaling 3 (SOC3), modulating chemokine

bioRxiv preprint doi: https://doi.org/10.1101/462929; this version posted November 5, 2018. The copyright holder for this preprint (which was not certified by peer review) is the author/funder, who has granted bioRxiv a license to display the preprint in perpetuity. It is made available under aCC-BY 4.0 International license.

production in intestinal epithelial cells and thereby avoiding intestinal inflammation in Crohn's disease, which may ultimately prevent the derived disease, CRC [37].

Since Metformin was able to revert the ACSL/SCD EMT phenotype, we tried to gain insight on this process using organoid cultures resembling the different stages of a CRC progression. Metformin treatment seems to be more efficient than 5-FU only during first tumor stages, making organoids recovery harder compared to the ones treated with 5-FU. We propose that Metformin therapies could be an appealing alternative in those cases when the tumor is detected in very early stages rather than 5-FU treatments. However, some studies of Metformin treatment in CRC patients points to stage III to be the most likeable to present an effect [38]. Since CRC is very improbable to detect on its very early stages, known as one of the most silent and deadly cancer; we wonder whether these studies with a low number of candidates in stage I are enough representative.

As well, Metformin therapies has been proposed alone or in combination with other drugs, in CRC. For example, Metformin has been recently combined with aspirin to treat middle stages in non-diabetic CRC patients.(II and III stages) [39]. Furthermore, it exists a Phase 2 Trial for the study of Metformin and 5-Fluorouracil combination in metastatic CRC [40] ,concluded with a longstanding cancer control. An older report also claimed the benefits of this combination, but they also reported that Metformin alone has antineoplastic activity *per se* in colon cancer cells, and enhanced the activity of 5-FU, oxaliplatin and irinotecan in cells previously treated [41].

Previous reports hypothesized that the inhibition of mitochondrial complex I was the main mechanism of action for Metformin. However, recent studies suggest that cancer progression is compromised upon Metformin treatment, by decreasing the TCA cycle´s anaplerosis. Metformin decreases the flow of glucose- and glutamine-derived metabolic intermediates into the TCA cycle, decreasing the citrate output of the mitochondria and leading to a reduction of acetyl-CoA (Ac-CoA) and oxaloacetate (OAA) in the cytoplasm and therefore a reduction in de novo FA synthesis [42]. This way, Metformin could be targeting lipid metabolism through ACSL/SCD axis. ACSL4

bioRxiv preprint doi: https://doi.org/10.1101/462929; this version posted November 5, 2018. The copyright holder for this preprint (which was not certified by peer review) is the author/funder, who has granted bioRxiv a license to display the preprint in perpetuity. It is made available under aCC-BY 4.0 International license.

404 downregulation in the presence of Metformin is clearly evident and the results are larger
405 significant in first stages (I, II) (Fig 4A). Maybe, the reduced overexpression of ACSL4 in the
406 first stages (Fig 1A) increases the sensitivity to Metformin action (Fig 4A); while in more
407 advanced stages, the overexpression is so high that Metformin action could appear to be less
408 effective. This would not be the case for SCD, which showed no overexpression in the first stages
409 and enhanced overexpression in III and IV stages, though it is significantly reduced upon
410 Metformin exposure again in the first stages (Fig 4B). On the other hand, it has been reported that
411 variations in the types and amounts of fatty acids, are able to modify intracellular ACSLs
412 expression [43], thus, this conditions could be also affecting ACSL/SCD components expression
413 besides that the network connection between those enzymes could make them present coordinated
414 effects upon Metformin treatment, reducing its expression due to the lack of their substrate.
415 Metformin was also previously reported to downregulate ACSL expression, lowering fatty acid
416 synthesis and normalizing lipid profile in diabetic rats [44]; as well as limiting its products, 18-
417 carbon chain length fatty acids, in skeletal muscle insulin resistant rats [45], suggesting in this
418 case that metformin is increasing FAs mitochondrial channeling due to the reduction of CPT1
419 inhibition by malonyl-CoA and therefore decreasing 18-carbon acyl-chain-derived bioactive
420 lipids in the cytoplasm [45], This action of Metformin could be additional to the aforementioned,
421 detoxifying ACSLs probable over activity.

422 Metformin seems also to target cancer stem cells of different cancer types [46]. However, we
423 have described for the first time the LGR5 downregulation in CRC-like organoids upon
424 Metformin treatment; consistent with previous reports using 2D CRC cultures [47]. LGR5 was
425 diminished in the whole CRC-like organoids series to minimum levels, an indicative that
426 Metformin action is affecting the stem cells of the crypt, responsible for the progression of the
427 organoids lineage. Curiously, Metformin treated organoids do not present apoptosis or even
428 necrosis, but they kept at a minimum size compared to other treatments, where the organoids layer
429 disappeared and the cells appeared apoptotic in the lumen (S6 Fig), showing that cell membrane
430 biogenesis is somehow blocked, mostly built by *de novo* lipogenesis routes.

bioRxiv preprint doi: https://doi.org/10.1101/462929; this version posted November 5, 2018. The copyright holder for this preprint (which was not certified by peer review) is the author/funder, who has granted bioRxiv a license to display the preprint in perpetuity. It is made available under aCC-BY 4.0 International license.

Finally, Metformin treated CRC organoids exhibit a greater compensatory increase in aerobic glycolysis. Since ATP levels are diminished due to complex I inhibition, the metabolic sensor AMPK is activated, inhibiting mTOR and proliferative events; and promoting glycolysis as an alternative ATP source [48]. We found that even though the CRC-organoids serie presented an increasing glycolysis with the stages, (Fig 5); Metformin was able to increase more this glycolytic phenotype, especially in stage I organoids, coincident with the higher sensitivity to the drug in this organoids. These results point towards Metformin targeting different metabolic routes other that Warburg effect to perform its effect on CRC organoids viability.

Even though the Warburg effect is a priority for current drugs, each day the evidence grows that other metabolic pathways should be targeted for cancer progression ablation. CRC is a leading cause of death in the developed world, though yet simplistic preclinical models that mimic the usual stages of CRC progression are lacking [13]. In this way, organoids further analysis need to be included as the tool of choice for stage-dependent drugs screening.

Conclusions

General conclusion

1. Organoids display a precise platform to assay **tumor stage-dependent drugs** being suitable for **personalized medicine**, constituting an invaluable tool due to their relatively low costs, animal saving suffering and their ease and legibility to genetically manipulate.

Metformin-related conclusions

2. **Metformin** treatment is further proved as an efficient drug in CRC:

   -It is able to decrease CRC-like organoids viability at the same rate as current chemotherapy (5-FU) but it does not affect to WT organoids.

bioRxiv preprint doi: https://doi.org/10.1101/462929; this version posted November 5, 2018. The copyright holder for this preprint (which was not certified by peer review) is the author/funder, who has granted bioRxiv a license to display the preprint in perpetuity. It is made available under aCC-BY 4.0 International license.

-Metformin treatment recovery is significantly inferior compared to 5-FU in **first stages organoids**, but with a greater recovery in WT organoids; becoming an appealing chemotherapy drug in first tumor phases.

-Metformin downregulates the stem cell biomarker LGR5 and Wnt target genes expression in all CRC-like organoid stages, reaffirming its potential use in intestinal cancers.

-Metformin action in CRC organoids is not related to a Warburg-effect impairment, presuming that other metabolisms rather than Warburg should be targeted to complete the cancer progression obstruction

ACSL/SCD-related conclusions

3. **ACSL4** is progressively overexpressed throughout CRC-like organoids stages; while **miR-19b-1-3p** preserves its protective role, reflecting the role of ACSL/SCD axis action on CRC progression. Besides, Metformin action is stronger on ACSL4 and SCD-overexpressing first stages organoids, agreeing with Metformin greater action on this stage.

bioRxiv preprint doi: https://doi.org/10.1101/462929; this version posted November 5, 2018. The copyright holder for this preprint (which was not certified by peer review) is the author/funder, who has granted bioRxiv a license to display the preprint in perpetuity. It is made available under aCC-BY 4.0 International license.

Acknowledgment

We kindly thank Dr. Daniel Stange and Dr. Schölch for providing the CRC-like organoids and to the whole Department of Gastrointestinal, Thoracic and Vascular Surgery at University Hospital Carl Gustav Carus for its continuous support .The research stay on this lab was kindly financed with the assistance of a Boehringer Ingelheim Fonds travel grant.

Conflict of interest statement

Authors declare no potential conflict of interest.

Source of funding

This work was supported by Ministerio de Economía y Competitividad del Gobierno de España (MINECO, Plan Nacional I+D+i AGL2016-76736-C3), Gobierno regional de la Comunidad de Madrid (P2013/ABI-2728, ALIBIRD-CM) and EU Structural Funds.

bioRxiv preprint doi: https://doi.org/10.1101/462929; this version posted November 5, 2018. The copyright holder for this preprint (which was not certified by peer review) is the author/funder, who has granted bioRxiv a license to display the preprint in perpetuity. It is made available under aCC-BY 4.0 International license.

References

1. Ferlay J, Soerjomataram I, Dikshit R, Eser S, Mathers C, Rebelo M, et al. Cancer incidence and mortality worldwide: sources, methods and major patterns in GLOBOCAN 2012. Int J Cancer. 2015;136: E359-386. doi:10.1002/ijc.29210

2. Müller MF, Ibrahim AEK, Arends MJ. Molecular pathological classification of colorectal cancer. Virchows Arch. 2016;469: 125–134. doi:10.1007/s00428-016-1956-3

3. Yamagishi, H., Kuroda, H., Imai, Y., & Hiraishi, H. (2016). Molecular pathogenesis of sporadic colorectal cancers. Chinese Journal of Cancer, 35, 4. http://doi.org/10.1186/s40880-015-0066-y

4. Fearon ER, Vogelstein B. A genetic model for colorectal tumorigenesis. Cell. 1990;61: 759–767.

5. Sánchez-Martínez R, Cruz-Gil S, Gómez de Cedrón M, Álvarez-Fernández M, Vargas T, Molina S, et al. A link between lipid metabolism and epithelial-mesenchymal transition provides a target for colon cancer therapy. Oncotarget. 2015;6: 38719–38736. doi:10.18632/oncotarget.5340

6. Nasri H, Rafieian-Kopaei M. Metformin: Current knowledge. J Res Med Sci Off J Isfahan Univ Med Sci. 2014;19: 658–664.

7. Baglia ML, Cui Y, Zheng T, Yang G, Li H, You M, et al. Diabetes Medication Use in Association with Survival among Patients of Breast, Colorectal, Lung, or Gastric Cancer. Cancer Res Treat Off J Korean Cancer Assoc. 2018; doi:10.4143/crt.2017.591

8. Cruz-Gil S, Sanchez-Martinez R, Gomez de Cedron M, Martin-Hernandez R, Vargas T, Molina S, et al. Targeting the lipid metabolic axisACSL/SCDin colorectal cancer progression by therapeutic miRNAs: miR-19b-1 role. J Lipid Res. 2018;59: 14–24. doi:10.1194/jlr.M076752

9. Sato T, Clevers H. SnapShot: Growing Organoids from Stem Cells. Cell. 2015;161: 1700–1700.e1. doi:10.1016/j.cell.2015.06.028

10. Werner K, Weitz J, Stange DE. Organoids as Model Systems for Gastrointestinal Diseases: Tissue Engineering Meets Genetic Engineering. Curr Pathobiol Rep. 2016;4: 1–9. doi:10.1007/s40139-016-0100-z

11. Sato T, Vries RG, Snippert HJ, van de Wetering M, Barker N, Stange DE, et al. Single Lgr5 stem cells build crypt-villus structures in vitro without a mesenchymal niche. Nature. 2009;459: 262–265. doi:10.1038/nature07935

12. Golovko D, Kedrin D, Yilmaz ÖH, Roper J. Colorectal cancer models for novel drug discovery. Expert Opin Drug Discov. 2015;10: 1217–1229. doi:10.1517/17460441.2015.1079618

bioRxiv preprint doi: https://doi.org/10.1101/462929; this version posted November 5, 2018. The copyright holder for this preprint (which was not certified by peer review) is the author/funder, who has granted bioRxiv a license to display the preprint in perpetuity. It is made available under aCC-BY 4.0 International license.

13. O'Rourke KP, Loizou E, Livshits G, Schatoff EM, Baslan T, Manchado E, et al. Transplantation of engineered organoids enables rapid generation of metastatic mouse models of colorectal cancer. Nat Biotechnol. 2017;35: 577–582. doi:10.1038/nbt.3837

14. Barker N, Huch M, Kujala P, van de Wetering M, Snippert HJ, van Es JH, et al. Lgr5(+ve) stem cells drive self-renewal in the stomach and build long-lived gastric units in vitro. Cell Stem Cell. 2010;6: 25–36. doi:10.1016/j.stem.2009.11.013

15. Boj SF, Hwang C-I, Baker LA, Chio IIC, Engle DD, Corbo V, et al. Organoid models of human and mouse ductal pancreatic cancer. Cell. 2015;160: 324–338. doi:10.1016/j.cell.2014.12.021

16. Huch M, Dorrell C, Boj SF, van Es JH, Li VSW, van de Wetering M, et al. In vitro expansion of single Lgr5+ liver stem cells induced by Wnt-driven regeneration. Nature. 2013;494: 247–250. doi:10.1038/nature11826

17. Sato T, Stange DE, Ferrante M, Vries RGJ, Van Es JH, Van den Brink S, et al. Long-term expansion of epithelial organoids from human colon, adenoma, adenocarcinoma, and Barrett's epithelium. Gastroenterology. 2011;141: 1762–1772. doi:10.1053/j.gastro.2011.07.050

18. Seidlitz T, Merker SR, Rothe A, Zakrzewski F, von Neubeck C, Grützmann K, et al. Human gastric cancer modelling using organoids. Gut. 2018; doi:10.1136/gutjnl-2017-314549

19. Barker N, Huch M, Kujala P, van de Wetering M, Snippert HJ, van Es JH, et al. Lgr5(+ve) stem cells drive self-renewal in the stomach and build long-lived gastric units in vitro. Cell Stem Cell. 2010;6: 25–36. doi:10.1016/j.stem.2009.11.013

20. Farin HF, Van Es JH, Clevers H. Redundant sources of Wnt regulate intestinal stem cells and promote formation of Paneth cells. Gastroenterology. 2012;143: 1518–1529.e7. doi:10.1053/j.gastro.2012.08.031

21. Andersson-Rolf A, Mustata RC, Merenda A, Kim J, Perera S, Grego T, et al. One-step generation of conditional and reversible gene knockouts. Nat Methods. 2017;14: 287–289. doi:10.1038/nmeth.4156

22. Bijsmans ITGW, Milona A, Ijssennagger N, Willemsen ECL, Ramos Pittol JM, Jonker JW, et al. Characterization of stem cell-derived liver and intestinal organoids as a model system to study nuclear receptor biology. Biochim Biophys Acta. 2017;1863: 687–700. doi:10.1016/j.bbadis.2016.12.004

23. Ciorba MA. Scap and the intestinal epithelial stem cell niche: new insights from lipid biology. J Lipid Res. 2015;56: 1381–1382. doi:10.1194/jlr.C061309

24. Chen W-C, Wang C-Y, Hung Y-H, Weng T-Y, Yen M-C, Lai M-D. Systematic Analysis of Gene Expression Alterations and Clinical Outcomes for Long-Chain Acyl-Coenzyme A Synthetase Family in Cancer. PLoS ONE. 2016;11. doi:10.1371/journal.pone.0155660

bioRxiv preprint doi: https://doi.org/10.1101/462929; this version posted November 5, 2018. The copyright holder for this preprint (which was not certified by peer review) is the author/funder, who has granted bioRxiv a license to display the preprint in perpetuity. It is made available under aCC-BY 4.0 International license.

565 25. Heimerl S, Moehle C, Zahn A, Boettcher A, Stremmel W, Langmann T, et al.
566 Alterations in intestinal fatty acid metabolism in inflammatory bowel disease.
567 Biochim Biophys Acta. 2006;1762: 341–350. doi:10.1016/j.bbadis.2005.12.006

568 26. Cao Y, Dave KB, Doan TP, Prescott SM. Fatty acid CoA ligase 4 is up-regulated
569 in colon adenocarcinoma. Cancer Res. 2001;61: 8429–8434.

570 27. Roongta UV, Pabalan JG, Wang X, Ryseck R-P, Fargnoli J, Henley BJ, et al.
571 Cancer cell dependence on unsaturated fatty acids implicates stearoyl-CoA
572 desaturase as a target for cancer therapy. Mol Cancer Res MCR. 2011;9: 1551–
573 1561. doi:10.1158/1541-7786.MCR-11-0126

574 28. Igal RA. Stearoyl CoA desaturase-1: New insights into a central regulator of
575 cancer metabolism. Biochim Biophys Acta. 2016;1861: 1865–1880.
576 doi:10.1016/j.bbalip.2016.09.009

577 29. Chen L, Ren J, Yang L, Li Y, Fu J, Li Y, et al. Stearoyl-CoA desaturase-1
578 mediated cell apoptosis in colorectal cancer by promoting ceramide synthesis. Sci
579 Rep. 2016;6: 19665. doi:10.1038/srep19665

580 30. Ran H, Zhu Y, Deng R, Zhang Q, Liu X, Feng M, et al. Stearoyl-CoA desaturase-1
581 promotes colorectal cancer metastasis in response to glucose by suppressing
582 PTEN. J Exp Clin Cancer Res CR. 2018;37: 54. doi:10.1186/s13046-018-0711-9

583 31. Qiu Y, Cai G, Zhou B, Li D, Zhao A, Xie G, et al. A distinct metabolic signature
584 of human colorectal cancer with prognostic potential. Clin Cancer Res Off J Am
585 Assoc Cancer Res. 2014;20: 2136–2146. doi:10.1158/1078-0432.CCR-13-1939

586 32. Lu Y, Zhou Z, Tao J, Dou B, Gao M, Liu Y. Overexpression of stearoyl-CoA
587 desaturase 1 in bone marrow mesenchymal stem cells enhance the expression of
588 induced endothelial cells. Lipids Health Dis. 2014;13: 53. doi:10.1186/1476-511X-
589 13-53

590 33. Tao J, Shi J, Lu Y, Dou B, Zhou Z, Gao M, et al. Overexpression of stearoyl-CoA
591 desaturase 1 in bone-marrow mesenchymal stem cells increases osteogenesis.
592 Panminerva Med. 2013;55: 283–289.

593 34. Wu Q, Yang Z, Wang F, Hu S, Yang L, Shi Y, et al. MiR-19b/20a/92a regulates
594 the self-renewal and proliferation of gastric cancer stem cells. J Cell Sci. 2013;126:
595 4220–4229. doi:10.1242/jcs.127944

596 35. Xiang J, Wu J. Feud or Friend? The Role of the miR-17-92 Cluster in
597 Tumorigenesis. Curr Genomics. 2010;11: 129–135.
598 doi:10.2174/138920210790886853

599 36. Zhang K, Zhang L, Zhang M, Zhang Y, Fan D, Jiang J, et al. Prognostic value of
600 high-expression of miR-17-92 cluster in various tumors: evidence from a meta-
601 analysis. Sci Rep. 2017;7: 8375. doi:10.1038/s41598-017-08349-4

602 37. Cheng X, Zhang X, Su J, Zhang Y, Zhou W, Zhou J, et al. miR-19b downregulates
603 intestinal SOCS3 to reduce intestinal inflammation in Crohn's disease. Sci Rep.
604 2015;5. doi:10.1038/srep10397

bioRxiv preprint doi: https://doi.org/10.1101/462929; this version posted November 5, 2018. The copyright holder for this preprint (which was not certified by peer review) is the author/funder, who has granted bioRxiv a license to display the preprint in perpetuity. It is made available under aCC-BY 4.0 International license.

605 38. Lee JH, Kim TI, Jeon SM, Hong SP, Cheon JH, Kim WH. The effects of
606 metformin on the survival of colorectal cancer patients with diabetes mellitus. Int J
607 Cancer. 2012;131: 752–759. doi:10.1002/ijc.26421

608 39. De Monte A, Brunetti D, Cattin L, Lavanda F, Naibo E, Malagoli M, et al.
609 Metformin and aspirin treatment could lead to an improved survival rate for Type
610 2 diabetic patients with stage II and III colorectal adenocarcinoma relative to non-
611 diabetic patients. Mol Clin Oncol. 2018;8: 504–512. doi:10.3892/mco.2018.1554

612 40. Miranda VC, Braghiroli MI, Faria LD, Bariani G, Alex A, Bezerra Neto JE, et al.
613 Phase 2 Trial of Metformin Combined With 5-Fluorouracil in Patients With
614 Refractory Metastatic Colorectal Cancer. Clin Colorectal Cancer. 2016;15: 321–
615 328.e1. doi:10.1016/j.clcc.2016.04.011

616 41. Effect of metformin alone and in combination with 5-fluorouracil (5FU),
617 oxaliplatin (O) and irinotecan (I) on human colon cancer cell lines.: Journal of
618 Clinical Oncology: Vol 29, No 15_suppl [Internet]. [cited 26 Jul 2018]. Available:
619 http://ascopubs.org/doi/abs/10.1200/jco.2011.29.15_suppl.e13041

620 42. Griss T, Vincent EE, Egnatchik R, Chen J, Ma EH, Faubert B, et al. Metformin
621 Antagonizes Cancer Cell Proliferation by Suppressing Mitochondrial-Dependent
622 Biosynthesis. PLoS Biol. 2015;13: e1002309. doi:10.1371/journal.pbio.1002309

623 43. Yan S, Yang X-F, Liu H-L, Fu N, Ouyang Y, Qing K. Long-chain acyl-CoA
624 synthetase in fatty acid metabolism involved in liver and other diseases: an update.
625 World J Gastroenterol. 2015;21: 3492–3498. doi:10.3748/wjg.v21.i12.3492

626 44. Ghadge A, Harsulkar A, Karandikar M, Pandit V, Kuvalekar A. Comparative anti-
627 inflammatory and lipid-normalizing effects of metformin and omega-3 fatty acids
628 through modulation of transcription factors in diabetic rats. Genes Nutr. 2016;11.
629 doi:10.1186/s12263-016-0518-4

630 45. Zabielski P, Chacinska M, Charkiewicz K, Baranowski M, Gorski J, Blachnio-
631 Zabielska AU. Effect of metformin on bioactive lipid metabolism in insulin-
632 resistant muscle. J Endocrinol. 2017;233: 329–340. doi:10.1530/JOE-16-0381

633 46. Metformin and Cancer Stem Cells: Old Drug, New Targets | Cancer Prevention
634 Research [Internet]. [cited 30 Jul 2018]. Available:
635 http://cancerpreventionresearch.aacrjournals.org/content/5/3/351

636 47. Mogavero A, Maiorana MV, Zanutto S, Varinelli L, Bozzi F, Belfiore A, et al.
637 Metformin transiently inhibits colorectal cancer cell proliferation as a result of
638 either AMPK activation or increased ROS production. Sci Rep. 2017;7: 15992.
639 doi:10.1038/s41598-017-16149-z

640 48. Andrzejewski S, Gravel S-P, Pollak M, St-Pierre J. Metformin directly acts on
641 mitochondria to alter cellular bioenergetics. Cancer Metab. 2014;2: 12.
642 doi:10.1186/2049-3002-2-12

643

bioRxiv preprint doi: https://doi.org/10.1101/462929; this version posted November 5, 2018. The copyright holder for this preprint (which was not certified by peer review) is the author/funder, who has granted bioRxiv a license to display the preprint in perpetuity. It is made available under aCC-BY 4.0 International license.

Supporting information

S1 Table. Primers´ sequences (Invivogen) used for quantitative real-time PCR.

S2 Table. Probes from TaqMan® MicroRNA Assays (ThermoFisher) used for quantitative real-time PCR.

S1 Fig. ACSL1 and SCD mRNA expression throughout CRC-like organoids stages

RT-QPCR analysis showing ACSL1 (A) and SCD (B) mRNA expression levels throughout CRC- like organoids stages. Results represent the fold-change mean ±SD (n = 3) (ns, $P > 0.05$; *, $P \leq 0.05$; **, $P \leq 0.01$; ***, $P \leq 0.001$; ****, $P \leq 0.0001$)

S2 Fig. ACSL/SCD regulatory miRNAs expression in CRC-like organoids

RT-QPCR analysis showing mRNA expression levels throughout CRC-like organoids stages of different ACSL/SCD regulatory miRNAS: miR-19b-1-5p (A), miR-142-3p (B), miR-142-5p (C). Results represent the fold-change mean ±SD (n = 3). (ns, $P > 0.05$; *, $P \leq 0.05$; **, $P \leq 0.01$; ***, $P \leq 0.001$; ****, $P \leq 0.0001$).

S3 Fig. Metformin and 5-FU effect in CRC-like organoids.

MTT cell viability assays upon 48 hours treatments with PBS (black bars), 10 uM Metformin (yellow bars) or 10, 100 and 150 uM 5-FU (grey bars) in the different CRC-like organoids representative stages: WT organoids (A); $APC^{fl/fl}$ organoids resembling stage I (B); $APC^{fl/fl}$, $KRAS^{G12D/WT}$ organoids resembling stage II (C); $APC^{fl/fl}$, $KRAS^{G12D/WT}$, $P53^{R172H/WT}$ organoids resembling stage III (D); $APC^{fl/fl}$, $KRAS^{G12D/WT}$,$P53^{R172H/WT}$,$Smad4^{fl/fl}$ organoids resembling stage IV (E). Data

bioRxiv preprint doi: https://doi.org/10.1101/462929; this version posted November 5, 2018. The copyright holder for this preprint (which was not certified by peer review) is the author/funder, who has granted bioRxiv a license to display the preprint in perpetuity. It is made available under aCC-BY 4.0 International license.

666 are represented by the fold-change mean ±SD (n = 3) in all the plots. (ns, $P > 0.05$; *, P
667 ≤ 0.05; **, $P \leq 0.01$; ***, $P \leq 0.001$; ****, $P \leq 0.0001$).

668

669 **S4 Fig. Metformin and 5-FU recovery effect in CRC-like organoids.**

670 MTT cell viability assays upon 48 hours treatments (black bars) and upon extra 72h post-
671 treatment recovery with PBS (light grey bars), 10 uM Metformin (yellow bars) or 10, 100
672 and 150 uM 5-FU (dark grey bars) in the different CRC-like organoids representative
673 stages:: WT organoids (A); *APC*$^{fl/fl}$ organoids resembling stage I (B); *APC*$^{fl/fl}$,
674 *KRAS*$^{G12D/WT}$ organoids resembling stage II (C); *APC*$^{fl/fl}$, *KRAS*$^{G12D/WT}$
675 ,*P53*$^{fl/R172H}$ organoids resembling stage III (D); *APC*$^{fl/fl}$, *KRAS*$^{G12D/WT}$
676 ,*P53*$^{fl/R172H}$,Smad4$^{fl/fl}$ organoids resembling stage IV (E). Data are represented by the
677 fold-change mean ±SD (n =3) in all the plots. (ns, $P > 0.05$; *, $P \leq 0.05$; **, $P \leq 0.01$;
678 ***, $P \leq 0.001$; ****, $P \leq 0.0001$).

679

680 **S5 Fig. ACSL/SCD axis and stem cell markers expression (Lgr5, Axin-2 and Ctnnb-**
681 **1) upon Metformin and 5-FU treatment**

682 Expression leveles of enzymes related to the ACSL/SCD axis, ACSL1 (A), ACSL4 (B)
683 and SCD (C) by RT-QPCR; and expression levels of different stem cell markers, Lgr5
684 (D), Axin-2 (E) and Ctnnb-1 (F) by RT-QPCR; upon PBS (black bars), 10 uM Metformin
685 (yellow bars) or 10, 100 and 150 uM 5-FU (grey bars). Data are represented by the fold-
686 change mean ±SD (n = 3). (ns, $P > 0.05$; *, $P \leq 0.05$; **, $P \leq 0.01$; ***, $P \leq 0.001$; ****,
687 $P \leq 0.0001$).

688

bioRxiv preprint doi: https://doi.org/10.1101/462929; this version posted November 5, 2018. The copyright holder for this preprint (which was not certified by peer review) is the author/funder, who has granted bioRxiv a license to display the preprint in perpetuity. It is made available under aCC-BY 4.0 International license.

689 **S6 Fig. Comparative organoids morphology between Metformin and other**
690 **oncologic treatments.**

691 Organoids (stage I and III) representative pictures with DMSO, Metformin and other
692 metabolic drugs against CRC progression, upon 48 hours treatments plus upon extra 72h
693 post-treatment recovery. Pictures were captured using the × 10 objective, in bright field.
694 Leica microscope (Leica microsystems).

695
696

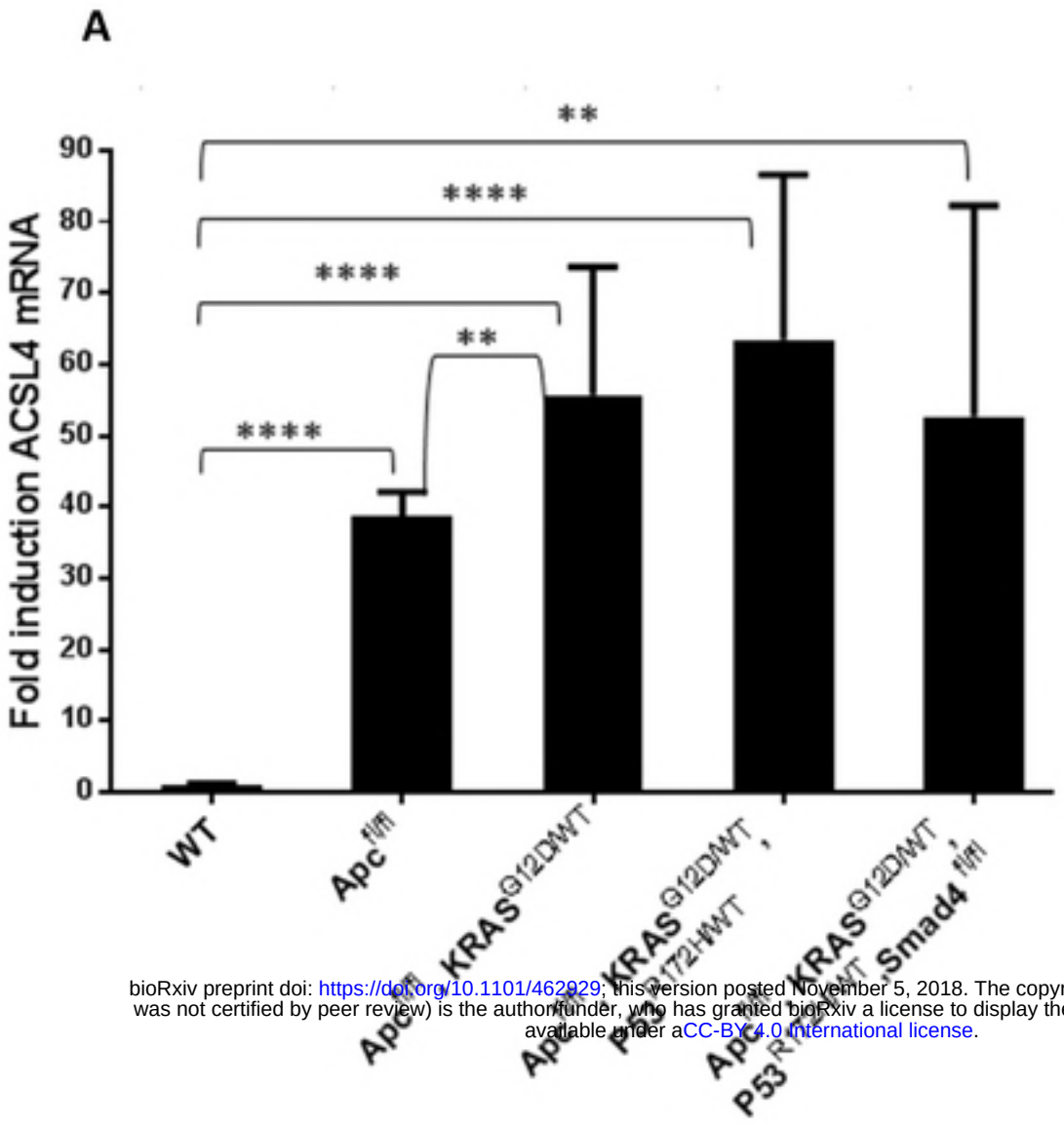

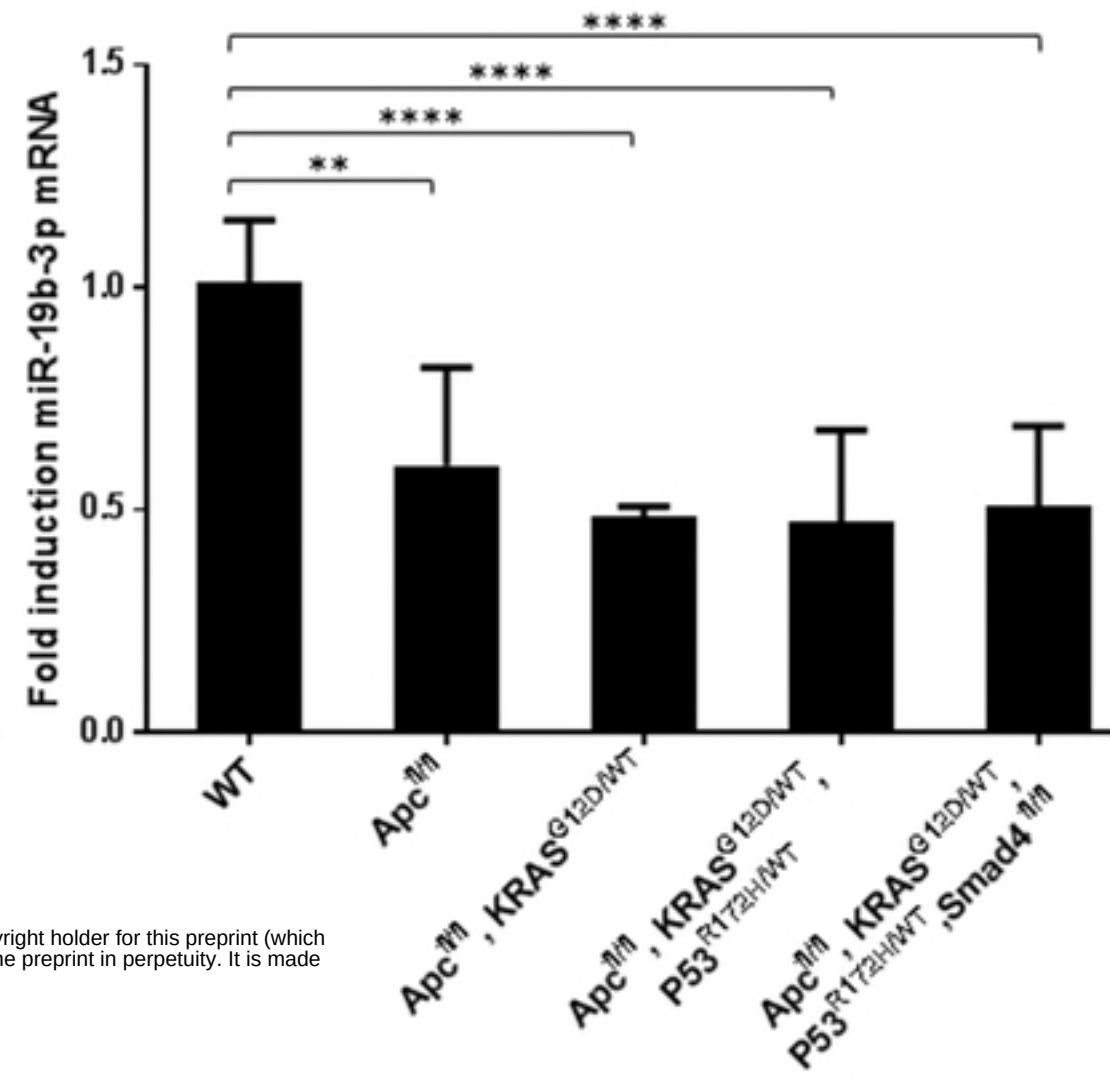

bioRxiv preprint doi: https://doi.org/10.1101/462929; this version posted November 5, 2018. The copyright holder for this preprint (which was not certified by peer review) is the author/funder, who has granted bioRxiv a license to display the preprint in perpetuity. It is made available under aCC-BY 4.0 International license.

Figure 1

bioRxiv preprint doi: https://doi.org/10.1101/462929; this version posted November 5, 2018. The copyright holder for this preprint (which was not certified by peer review) is the author/funder, who has granted bioRxiv a license to display the preprint in perpetuity. It is made available under aCC-BY 4.0 International license.

A

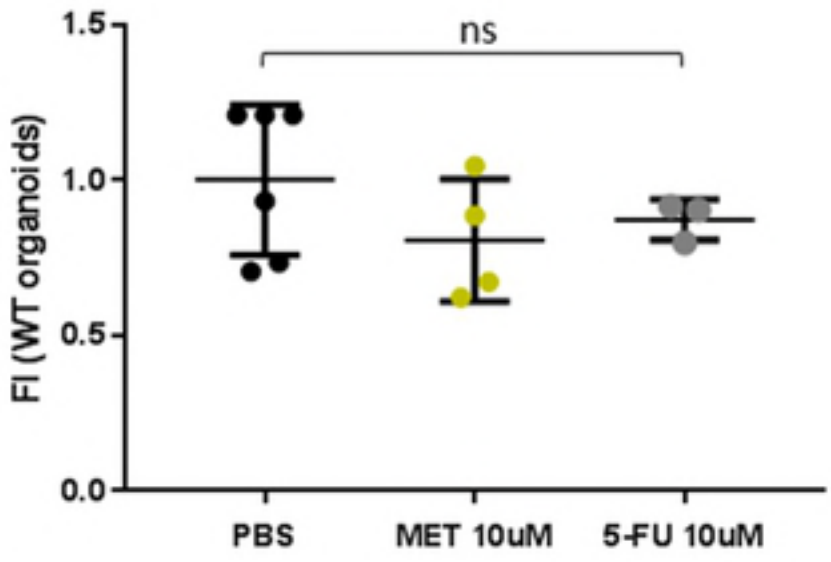

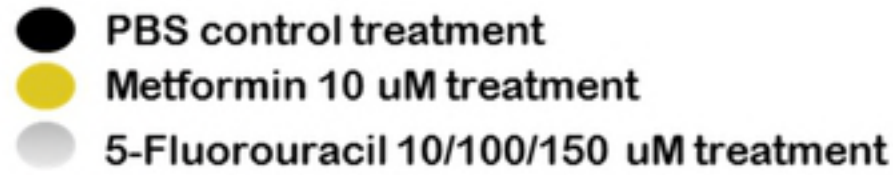

B

C

D

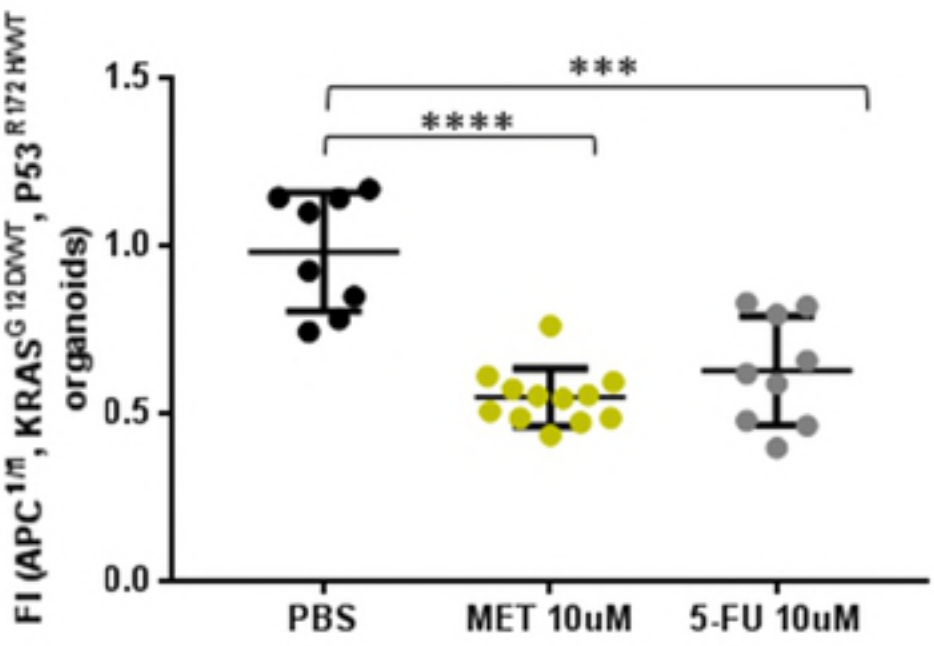

E

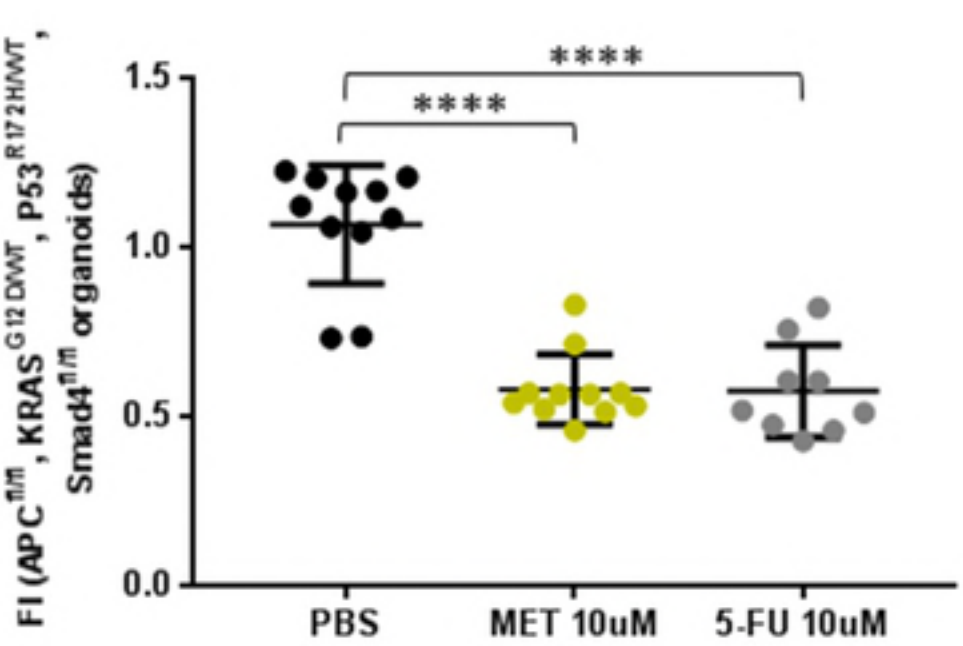

Figure 2

Figure 3

bioRxiv preprint doi: https://doi.org/10.1101/462929 version posted Nove 5, 2018. The copyright holder for this preprint (w
was not certified by pe ew) is the author/fun o has granted bioRx ense to display the preprint in perpetuity. It s m
availab er aCC-BY 4.0 International license.

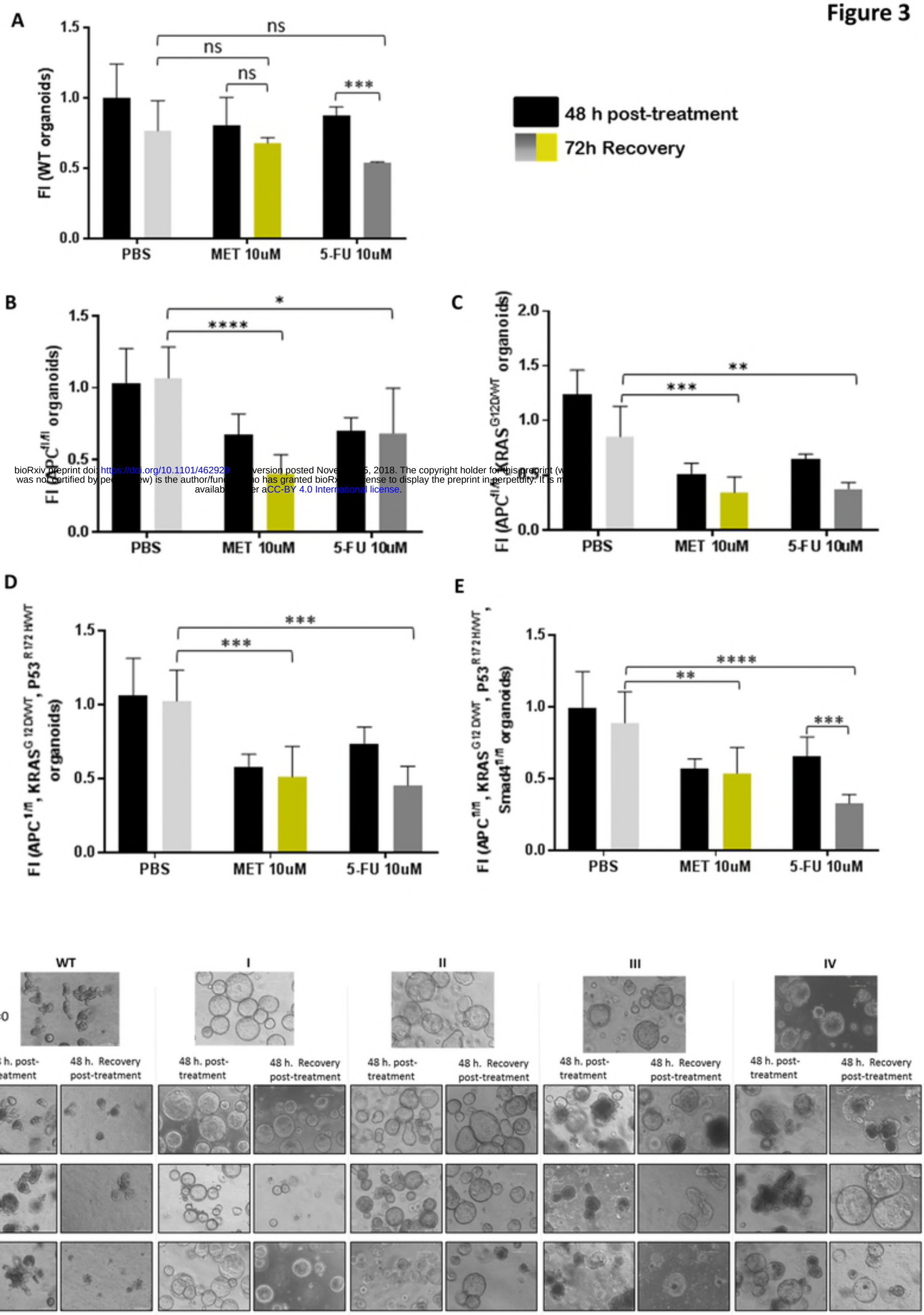

Figure 3

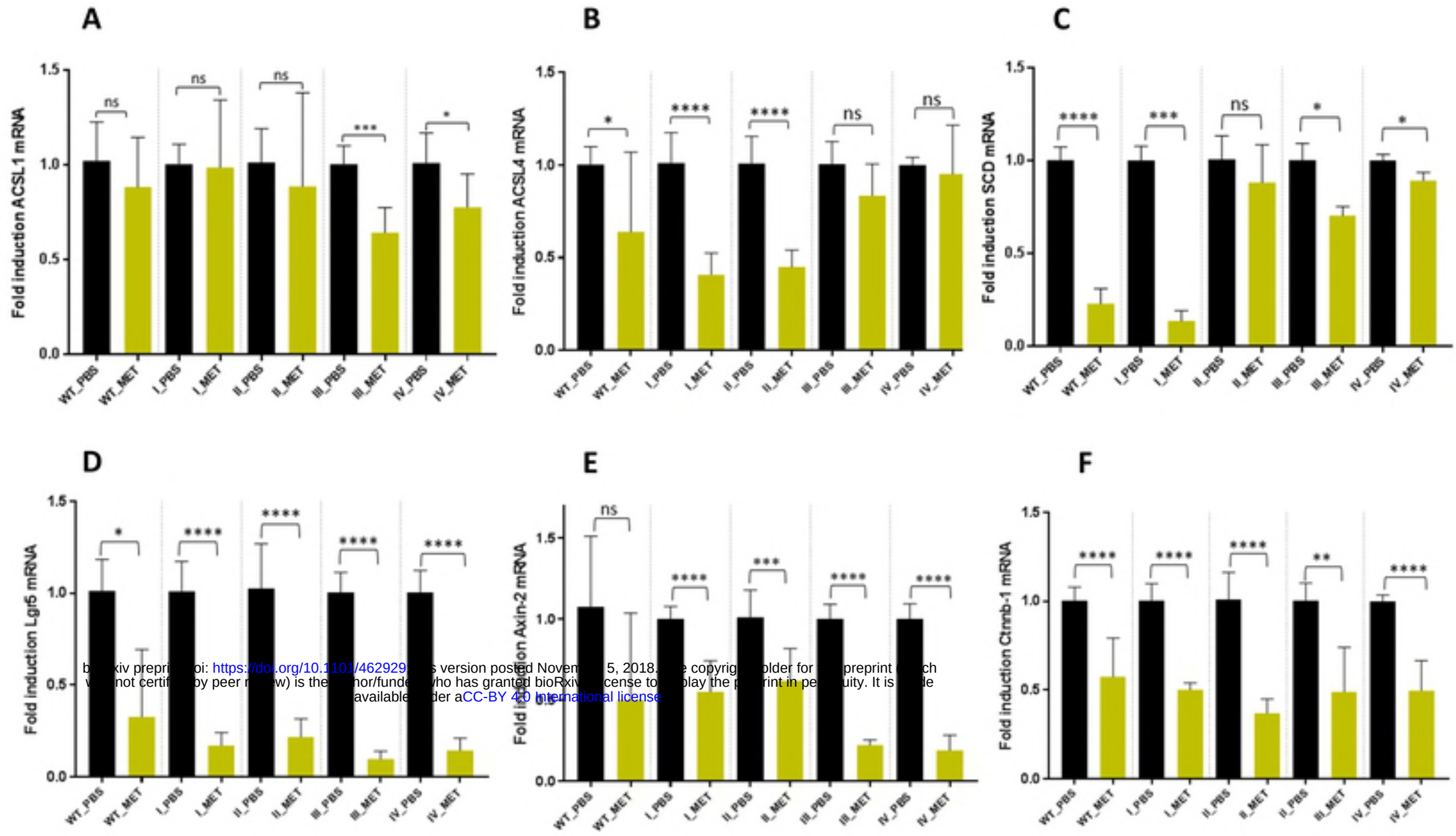

bioRxiv preprint doi: https://doi.org/10.1101/462929 this version posted November 5, 2018. The copyright holder for this preprint (which was not certified by peer review) is the author/funder, who has granted bioRxiv a license to display the preprint in perpetuity. It is made available under aCC-BY 4.0 International license.

Figure 4

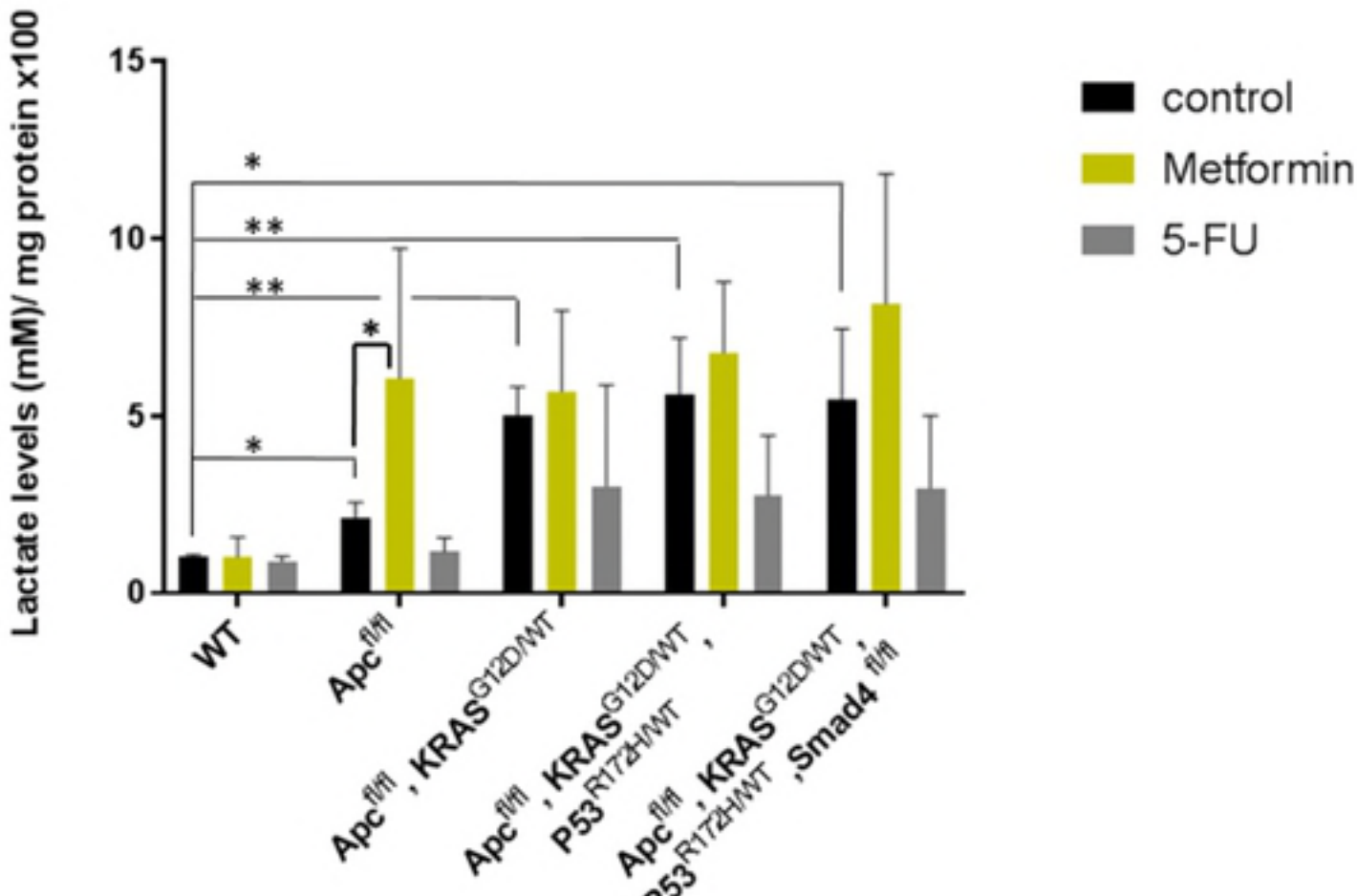

bioRxiv preprint doi: https://doi.org/10.1101/462929; this version posted November 5, 2018. The copyright holder for this preprint (which was not certified by peer review) is the author/funder, who has granted bioRxiv a license to display the preprint in perpetuity. It is made available under aCC-BY 4.0 International license.

Figure 5